

# Zhongfeng Xingnao Liquid Ameliorated the Early Impairment of Intracerebral Hemorrhage by Inhibiting NF- $\kappa$ B/NLRP3 Axis in Rats

Heyu Yang<sup>1-3,\*</sup>, Bingqian Luo<sup>1-3,\*</sup>, Yifan Du<sup>3,4,\*</sup>, Jiafu Guo<sup>1-3</sup>, Shiqi Zhang<sup>1-3</sup>, Ping Wang<sup>1-3</sup>, Yuan Dai<sup>3,4</sup>, Yun Lu<sup>3,5</sup>, Shijun Xu<sup>1-3</sup>

<sup>1</sup>State Key Laboratory of Southwestern Chinese Medicine Resources, Chengdu University of Traditional Chinese Medicine, Chengdu, Sichuan, 611137, People's Republic of China; <sup>2</sup>School of Pharmacy, Chengdu University of Traditional Chinese Medicine, Chengdu, Sichuan, 611137, People's Republic of China; <sup>3</sup>Institute of Material Medica Integration and Transformation for Brain Disorders, Chengdu University of Traditional Chinese Medicine, Chengdu, Sichuan, 611137, People's Republic of China; <sup>4</sup>School of Health Preservation and Rehabilitation, Chengdu University of Traditional Chinese Medicine, Chengdu, Sichuan, 611137, People's Republic of China; <sup>5</sup>Hospital of Chengdu University of Traditional Chinese Medicine, Chengdu, Sichuan, 610072, People's Republic of China

\*These authors contributed equally to this work

Correspondence: Yun Lu; Shijun Xu, Email luyun999@126.com; xushijun@cdutcm.edu.cn

**Background:** Perihematomal neuroinflammation serves as a pivotal pathogenic driver of secondary brain injury during the acute stage of intracerebral hemorrhage (ICH). The traditional Chinese medicine Zhongfeng Xingnao Liquid exhibits anti-neuroinflammatory effects. This study aims to elucidate the optimal timing for ZFXN administration within hours of symptom onset and its underlying mechanisms, focusing on NF- $\kappa$ B/NLRP3-mediated neuroinflammation.

**Methods:** ICH was induced by injection of autologous arterial blood into the left caudal nucleus. Neurological deficits scores, hematoma volume, cerebral blood flow (CBF), H&E and Nissl staining were conducted at 24 hours following ICH. The levels of neuroinflammation response and NF- $\kappa$ B/NLRP3 axis surrounding the hematoma were measured using immunofluorescent staining and Western blot. The inhibition of ZFXN on NF- $\kappa$ B/NLRP3 axis was further confirmed in Lipopolysaccharide (LPS)-induced BV-2 cells.

**Results:** Post-ICH pathology was characterized by progressive hematoma expansion, elevated neurological deficit scores, neuronal damage, and reduced CBF, accompanied by neuroinflammation. Early ZFXN intervention within 6 hours post-ICH significantly reduced hematoma volume and improved neurological scores (mNSS, Bederson, Zea Longa) at 24 hours, while markedly alleviating perihematomal neuronal damage and enhancing CBF, with optimal efficacy observed following one-hour administration. The treatment also effectively suppressed IL-1 $\beta$ /TNF- $\alpha$  release and microglial activation through NF- $\kappa$ B/NLRP3 pathway inhibition. Consistently, ZFXN diminished NF- $\kappa$ B-p65 nuclear translocation and downregulated NLRP3 inflammasome components (ASC, Cleaved Caspase-1) in LPS-stimulated BV-2 cells.

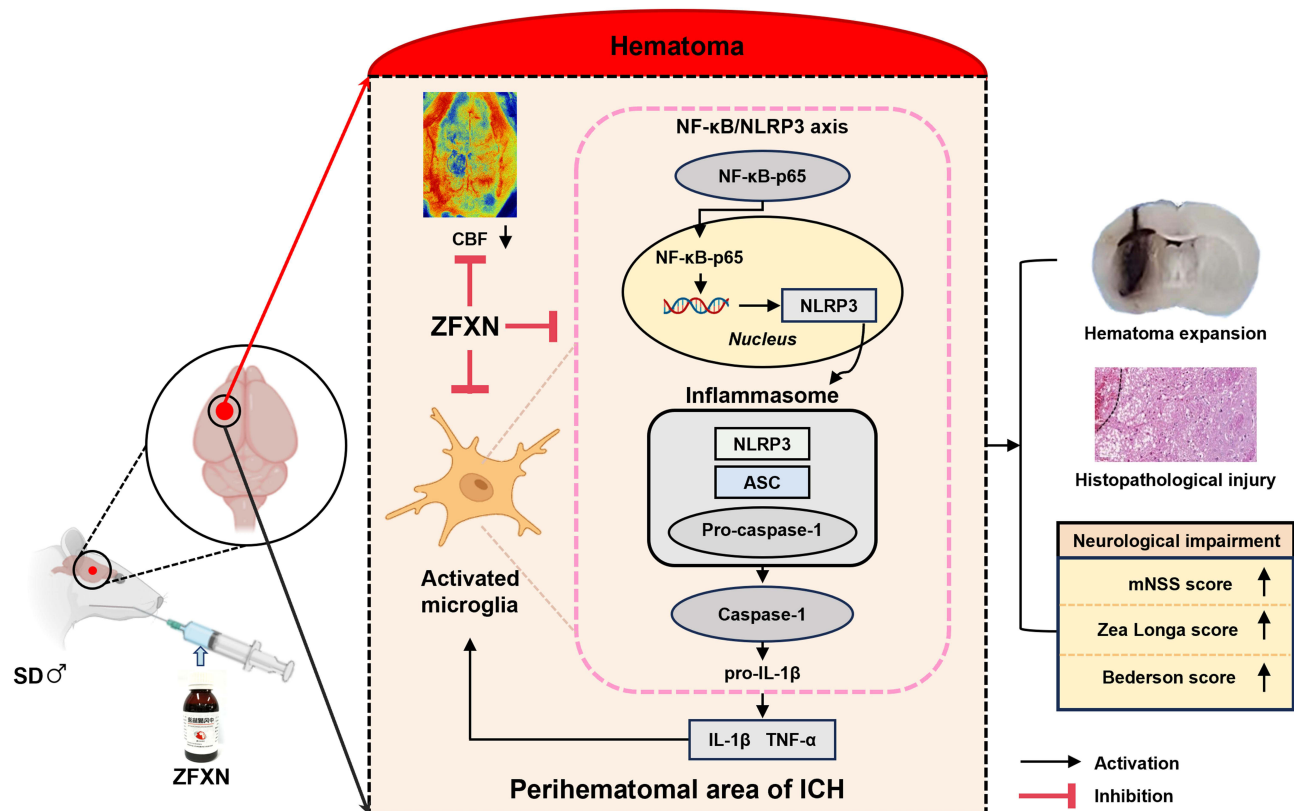
**Conclusion:** ZFXN emerges as a promising neuroprotective agent for ICH through targeted inhibition of the NF- $\kappa$ B/NLRP3 inflammatory axis, demonstrating optimal efficacy within the critical 6-hour hyperacute phase by mitigating secondary neuroinflammation and addressing current therapeutic gaps in ICH management.

**Keywords:** Zhongfeng Xingnao liquid, intracerebral hemorrhage, neuroinflammation, microglia, NF- $\kappa$ B/NLRP3 axis

## Introduction

Intracerebral hemorrhage (ICH) represents the most fatal subtype of stroke, accounting for 10–30% of all stroke cases.<sup>1,2</sup> Despite advancements in hyperacute care bundle approach, early minimal invasive hematoma evacuation and the use of Xa-inhibitor, the survival rate after one year remains low, with significant sequelae among survivors.<sup>3–6</sup> Hematoma volume and subsequent expansion are strongly associated with the early neurological deterioration and overall outcomes in ICH patients.<sup>7</sup> Consequently, early interventions within hours of presentation are deemed essential to reducing disability and death following acute ICH.<sup>8</sup>

## Graphical Abstract



The occurrence of ICH initiates both primary and secondary injuries. Hematoma formation following ICH leads to elevated intracranial pressure and diminished peripheral cerebral blood flow (CBF), which results in cerebral ischemia and neuronal death.<sup>9,10</sup> The subsequent lysis and degradation of red blood cells release neurotoxic degradation products, such as hemoglobin and peroxidase, which induce neuroinflammation through activating microglia and result in secondary brain impairment.<sup>11</sup> Approximately 20% patients experience hematoma expansion within 24 hours of ICH onset, closely linked to neuroinflammation driven by activated microglia in the perihematomal region.<sup>12,13</sup> The enlarged hematoma and neuroinflammation together contribute to approximately 23% early neurological deficits, which attribute to neuronal damage surrounding the hematoma.<sup>14</sup> Inhibition microglial activation not only curtails hematoma expansion but also mitigates subsequent neuroinflammation, thereby relieving neuronal damage and neurological dysfunction. This suggests that targeting neuroinflammation may present a window of opportunity for alleviating neurological injury in the early stages of ICH.<sup>15,16</sup> Activated nuclear factor-κB (NF-κB)/NOD-LRR- and pyrin domain-containing 3 (NLRP3) axis is crucial for the pro-inflammatory cascade around hematoma at early stage of ICH.<sup>17</sup> Numerous studies have demonstrated that inhibition the NF-κB/NLRP3 axis is beneficial for the early brain injury and neuroinflammation following ICH.<sup>18</sup> NF-κB is rapidly activated within 1–6 hours following ICH, orchestrating the initiation phase of the inflammatory cascade by regulating the transcriptional activation of key genes including NLRP3. Recent mechanistic studies further validate the therapeutic potential of targeting this axis. Notably. Administration of ZFXN in ICH mouse models resulted in a marked reduction in NLRP3 production, demonstrating its capacity to attenuate the progression of the inflammatory response following ICH.<sup>19</sup> Ursolic Acid Alleviates Neuroinflammation after Intracerebral Hemorrhage by Mediating the apoptosis of microglia via the NF-κB/NLRP3/GSDMD Pathway.<sup>20</sup>

Currently, no specific treatment exists for ICH. Some traditional Chinese medicines prescriptions have shown potential benefits in animal models and early clinical trials,<sup>9</sup> but recent advances lead to cautious optimism regarding their efficacy. Zhongfeng Xingnao Liquid (ZFXN),<sup>21</sup> an oral prescription derived from Renshen-Dahuang Decoction in *Bian-zheng-lu*, comprises 30 parts Renshen (*Panax ginseng* C. A. Mey), 15 parts Chuanxiong (*Ligusticum chuanxiong* hort.), 10 parts Sanqi (*Panax notoginseng* (Burk.) F.H. Chen), and 5 parts Dahuang (*Rheum palmatum* L). ZFXN's neuroprotective efficacy derives from its synergistic multi-component composition: Salvianolic acid B (demonstrated microglial activation inhibition via TLR4/NF- $\kappa$ B pathway modulation),<sup>22</sup> Ferulic acid (established free radical scavenging and antioxidant properties through Nrf2 activation).<sup>23</sup> This unique combination simultaneously targets both neuroinflammation and oxidative stress - the two predominant pathological mechanisms underlying ICH-induced secondary brain injury.

ZFXN has been utilized in clinical settings for over 20 years to treat ICH. However, the long-term outcomes of ZFXN on the prognosis of ICH patients have yielded inconsistent results in two multicentre, randomised, double-blind, clinical trial, where treatment commenced 48-hours following ICH. In pre-specified subgroup analyses of a large-scale randomized, placebo-controlled, double-blind trial, patients with ICH volumes exceeding 15 mL and those with lobar hemorrhage demonstrated signals of potential therapeutic benefit. Concurrently, mild diarrhea symptoms were observed in patients administered by ZFXN.<sup>24,25</sup> It is well established that hematoma expansion predominantly occurs within the first three hours after ICH, affecting approximately one-fourth to one-third of patients.<sup>12,26</sup> The volume and duration of cerebral hematoma are closely related to neuronal impairment surrounding hematoma and worse outcomes. No FDA-approved neuroprotective agents exist for hyperacute phase intervention (<6h post-ictus); Clinical management remains predominantly supportive (blood pressure control) or surgical (hematoma evacuation). The crucial early therapeutic window for preventing secondary injury remains unaddressed by current therapies. This underscores the urgent need for precisely timed, mechanism-targeted interventions like ZFXN that can modulate the early inflammatory cascade. Therefore, it is imperative to investigate whether ultra-early intervention with ZFXN can optimize near-term outcomes in early ICH. This work evaluated the therapeutic effects of ZFXN administered at various time points within 12 hours post ICH in a rat model, focusing on its promising mechanisms related to neuroinflammation mediated by NF- $\kappa$ B/NLRP3 axis.

## Materials and Methods

### Experimental Drugs and Reagent

Zhongfeng Xingnao Liquid (NO. 20230912, ZFXN, 0.96 g raw medicinal materials/mL, 50mL/d for ICH patients) was sourced from Hospital of Chengdu University of Traditional Chinese Medicine (Chengdu, China). LPS (L2630) and Pentobarbital sodium (69020100) were procured from Merck KGaA (Darmstadt, Germany). Hematoxylin-Eosin (H&E) staining solution (G1001), Nissl staining solution (G1004) and Hoechst 33258 staining solution were purchased from Servicebio (Wuhan, China). The cell counting Kit-8 (BG0025), and Nuclear and Cytoplasmic Protein Extraction Kit (BL670A) were provided by Biosharp (Hefei, China). Anti-IL-1 $\beta$  (AB234437, Abcam, Cambridge, Britain), Anti-TNF- $\alpha$  (11948S) and Anti-Cleaved Caspase-1 (89332S) were obtained from Cell Signaling Technology (Danvers, America). Anti-NF- $\kappa$ B p65 (AF5006) and Anti-NLRP3 (DF7438) were procured from Affinity (Changzhou, China). Anti-ASC (A22046, Abclonal, Wuhan, China). Anti- $\beta$ -Actin (GB15003, Servicebio). Anti-Histone H3.1 (P30266, ABMART, Shanghai, China). HRP-conjugated goat anti-mouse IgG (GB23301), HRP-conjugated goat anti-rabbit IgG (GB23303), Alexa Fluor<sup>®</sup> 488-conjugated goat anti-rabbit IgG (GB25303), Cy3-conjugated goat anti-mouse IgG (GB21301), all sourced from Servicebio, along with multimeric anti-mouse IgG-HRP (SV0001, Boster, Wuhan, China).

### Animals' Protocols

Healthy male Sprague-Dawley rats (SPF grade, 7–8 weeks old, body weight 280 $\pm$ 40 g) were acquired Sichuan Weitong Lihua Laboratory Animal Technology Co., Ltd. (No.511215600001218). Rats were housed in an SPF animal facility (22 $\pm$ 2°C, 50–60% humidity, and a 12-hour light/dark cycle) with ad libitum access to food and water. The animal protocols

received approval from the Laboratory Animal Ethics Committee of Chengdu University of Traditional Chinese Medicine (Approval No. 2023001, November 7, 2023). All animals' protocols were strictly conducted following the Care and Use of Laboratory Animals by the National Academy of Sciences (8th edition). Rats were randomly assigned to Sham, ICH, and three intervention groups treated with ZFXN at 1-, 6- and 12-hours post-ICH, respectively, designated as ZFXN-1, ZFXN-6 and ZFXN-12 (n=10 per group). The ICH model was established by injecting 100  $\mu$ L autologous tail artery blood into the left caudal nucleus, while the Sham group underwent surgical procedures without blood injection. The injected blood volume corresponded to an 80 mL ICH volume in humans.<sup>27</sup> Injection coordinates were set at 3 mm left, 0.2 mm posterior to Bregma, and 6 mm below the cortical surface.<sup>28</sup> Rats in ZFXN-1, ZFXN-6 and ZFXN-12 group were oral administered with 7 mL/kg ZFXN at 1-, 6- and 12-hours post-surgery, respectively. The dose of ZFXN was determined based on clinical dosage conversion.<sup>21</sup> Behavioral assessments and CBF measurements were conducted 24 hours after surgery, after which animals were euthanized, and brain tissue and serum were collected for subsequent analyses.

## Neurological Function Evaluation

Neurological functions of rats were assessed 24-hours post-blood injection using the Modified Neurological Severity Score (mNSS) test, along with the Zea Longa score and the Bederson score.<sup>29–31</sup> mNSS Score: Neurological deficits were evaluated by motor tests (postural asymmetry), beam balance (equilibrium), sensory tests (tactile/pain response), reflexes (pinna/corneal), and abnormal movements (tremors/seizures) (Table S1), with a total score of 0–18 (mild: 0–6, moderate: 7–12, severe: 13–18). Zea Longa Score: Grading focused on spontaneous activity severity: contralateral limb flexion (1 point), circling (2 points), tumbling (3 points), no movement (4 points), and death (5 points) (Table S2), with a total score of 0–5 (no deficit: 0, mild: 1–2, severe: 3–5). Bederson Score: Assessments included spontaneous activity (reduced movement), body symmetry (contralateral limb flexion), forelimb extension (failure to extend), resistance to lateral push (asymmetric strength), and climbing ability (grasping impairment) (Table S3), scored 0–3 (normal: 0, moderate: 1, severe: 2–3).

## Cerebral Blood Flow (CBF) Measurement

Following behavioral assessments, rats were anesthetized with 3% pentobarbital sodium, and the skull was fully exposed. CBF was monitored using a laser speckle flow imaging system (RFLSI ZW, RWD Life Science, Shenzhen, China). Data analysis was performed using RFLSI Analysis V 2.1.3.34859 software, and mean perfusion and pseudo-color images were extracted during stable blood flow periods.

## Hematoma Volume and Pathological Staining of Rat's Brain Tissue

After 24 hours of fixation, brain tissue was uniformly sectioned into seven consecutive 2 mm thick slices using a brain slice mold, and images were captured under consistent lighting conditions. The brain hematoma volume was calculated using Tada's formula. For HE staining, brain tissue underwent dehydration, paraffin embedding, and sectioning, followed by staining with H&E staining solution, Nissl staining solution, and immunohistochemistry staining reagents, with subsequent scanning using a scanner (TP1020/CM1950, Sunny Optical Technology (group) Co., Ltd., Hong Kong, China). Pathological staining images were subsequently analyzed using Aperio Image Scope software.

## CCK8 Assay

The BV-2 cell line was purchased from the Kunming Cell Bank, Chinese Academy of Sciences. Cells were cultured in DMEM high-glucose medium containing 10% fetal bovine serum at 37°C and 5% CO<sub>2</sub>. After BV-2 cells were seeded in a 96-well plate for 24 hours, and the treat with Lipopolysaccharide (LPS) for 12 hours, various concentrations of ZFXN were administered for 12 hours to assess its effects on cell viability using CCK8.



## Western Blot (WB)

Protein samples were extracted from brain tissue surrounding the hematoma or from BV-2 cells. Total proteins were measured by a BCA kit, followed by separation via SDS-PAGE and transferred to a PVDF membrane. The membrane was blocked for 1 hour and subsequently incubated with the primary antibodies overnight at 4°C, followed by a 1-hour incubation with the secondary antibody at room temperature. Imaging was performed using a chemiluminescence imaging system with enhanced chemiluminescence reagent (Touch Imager Pro, E-Blot, Shanghai, China). All primary antibodies used in Western blot (WB) were diluted at a ratio of 1:1000.

## Immunofluorescence (IF) Analysis

IF procedures began with the deparaffinization and hydration of paraffin sections, which were subsequently blocked with goat serum. The primary antibody was applied overnight at 4°C, followed by a 1-hour incubation with fluorescent secondary antibodies at room temperature in the dark. Nuclei were stained with Hoechst, and the slices were sealed with an anti-fluorescence quenching agent. BV-2 cells were seeded on cell slides within 24-well plates, fixed with 4% paraformaldehyde after modeling and ZFXN administration, and underwent the same blocking and antibody incubation procedures as the tissue sections. Imaging was conducted using a fluorescence microscope (TP1020/CM1950, Sunny Optical Technology (Group) Co., Ltd., Hong Kong, China).

## Statistical Analysis

Statistical analyses were performed using one-way analysis of variance (ANOVA), with data expressed as Mean  $\pm$  SEM. For comparisons among groups, one-way ANOVA followed by Tukey's multiple comparisons test was applied if normality and homogeneity of variance assumptions were met. If these assumptions were violated, the Kruskal–Wallis non-parametric test with Dunn's post hoc analysis was used. Statistical significance was defined as  $p < 0.05$ .

## Results

### ZFXN Reduced Neurological Deficit Scores and Hematoma Volume in ICH Rats

Animal protocols were illustrated in [Figure 1A](#). Data indicated ICH rats exhibited higher neurobehavioral scores in mNSS, Zea Longa and Bederson tests compared to Sham rats, alongside an increased volume of cerebral hematoma ([Figure 1B–F](#)). Early intervention with ZFXN at one-hours and six-hours post-ICH significantly decreased the neurobehavioral scores and hematoma volume in ICH rats, while no distinct effects observed at twelve-hours ([Figure 1B–F](#)). Interestingly, the most pronounced therapeutic effect was recorded when ZFXN was administered one-hour post-surgery, suggesting ultra-early administration of ZFXN within six-hours following ICH may confer the greatest benefit to ICH short-term outcomes.

### ZFXN Alleviated Neurological Impairment Induced by ICH in Rats

The reduction of peripheral CBF is a critical aspect of ICH, closely related to adverse outcomes in patients.<sup>32</sup> Laser speckle imaging demonstrated that CBF in ICH rats was significantly lower than that in Sham rats, while ZFXN treatment markedly increased CBF in ZFXN-1 and ZFXN-6 rats ([Figure 2A and B](#)). H&E results showed a significant histopathological impairment in the regional brain tissue surrounding the hematoma post-ICH, including disordered neuronal arrangements, nuclear pyknosis and inflammatory cell infiltration. However, those changes were significantly mitigated by ZFXN administration at one-hour and six-hour post-ICH, particularly with the one-hour treatment ([Figure 2C](#)). Similar findings were found in Nissl staining, which indicated a higher number of Nissl bodies in ZFXN-treated rats compared to ICH rats, especially in ZFXN-1 group ([Figure 2D](#)). These findings imply the ultra-early intervention with ZFXN alleviates neuronal damage surrounding the hematoma by facilitating CBF in ICH rats.

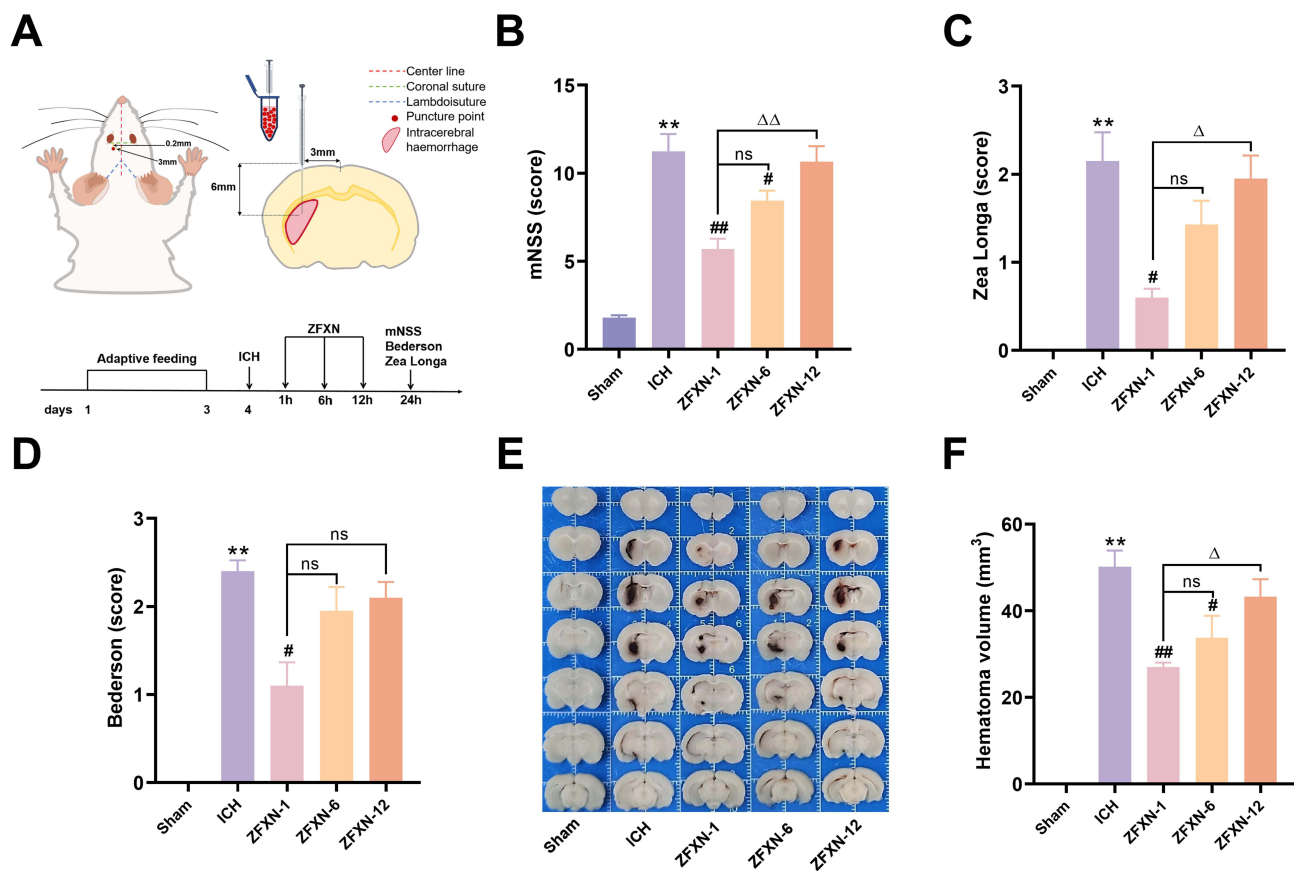


**Figure 1** ZFXN reduced neurological deficit scores and hematoma volume in ICH rats. **(A)** Experimental protocol flowchart. **(B)** mNSS scores (n=10). **(C)** Zea Longa scores (n=10). **(D)** Bederson scores (n=10). **(E)** Representative coronal brain tissue sections. **(F)** Hematoma volume ratio (n=5). \*\*p<0.01 vs Sham rats; #p<0.05, ##p<0.01 vs ICH rats;  $\Delta$ p<0.05,  $\Delta\Delta$ p<0.01 vs ZFXN-1 rats; ns indicates no significant difference (p≥0.05).

## ZFXN Inhibited Microglial Activation Around the Hematoma in ICH Rats

Based on the forementioned findings, ZFXN-1 was selected for further mechanistic exploration. Neuroinflammatory driven by microglia activation in the peri-hematoma area is a crucial factor influencing the extent of ICH-related impairment.<sup>33–35</sup> Immunohistochemical and IF analyses revealed a significant increase in Iba1<sup>+</sup> cells density surrounding hematoma in ICH rats, characterized by swollen cell bodies and the absence of processes. However, treatment with ZFXN markedly reduced the density of Iba1-positive cells and restored the normal morphology of microglia (Figure 3A–D). Additionally, the expression of Iba1 protein was higher around the hematoma of ICH rats than that of in Sham rats, whereas, ZFXN treatment significantly inhibited Iba1 levels (Figure 3E). These results hint ZFXN reduces neuroinflammatory surrounding hematoma of ICH by inhibiting microglia activation.

## ZFXN Suppressed Inflammatory Cytokines in the Perihematoma Area of ICH Rats

The release and invasion of inflammatory cytokines are significant contributors to neuronal death, and anti-inflammatory strategies are currently a focal area of research during the acute stages of ICH.<sup>36,37</sup> Our data showed that the IF intensity of interleukin-1 $\beta$  (IL-1 $\beta$ ) in the peri-hematoma area was markedly inhibited in ZFXN-1 rats compared with ICH rats (Figure 4A and B). Similarly, the expression of IL-1 $\beta$  and Tumor necrosis factor alpha (TNF- $\alpha$ ) in the perihematoma area of ICH rats were significantly higher than that of in Sham rats, but markedly reduced following ZFXN treatment (Figure 4C and D). These results indicate ZFXN inhibits the release and invasion of inflammatory cytokines surrounding hematoma when administered orally one hour after ICH.

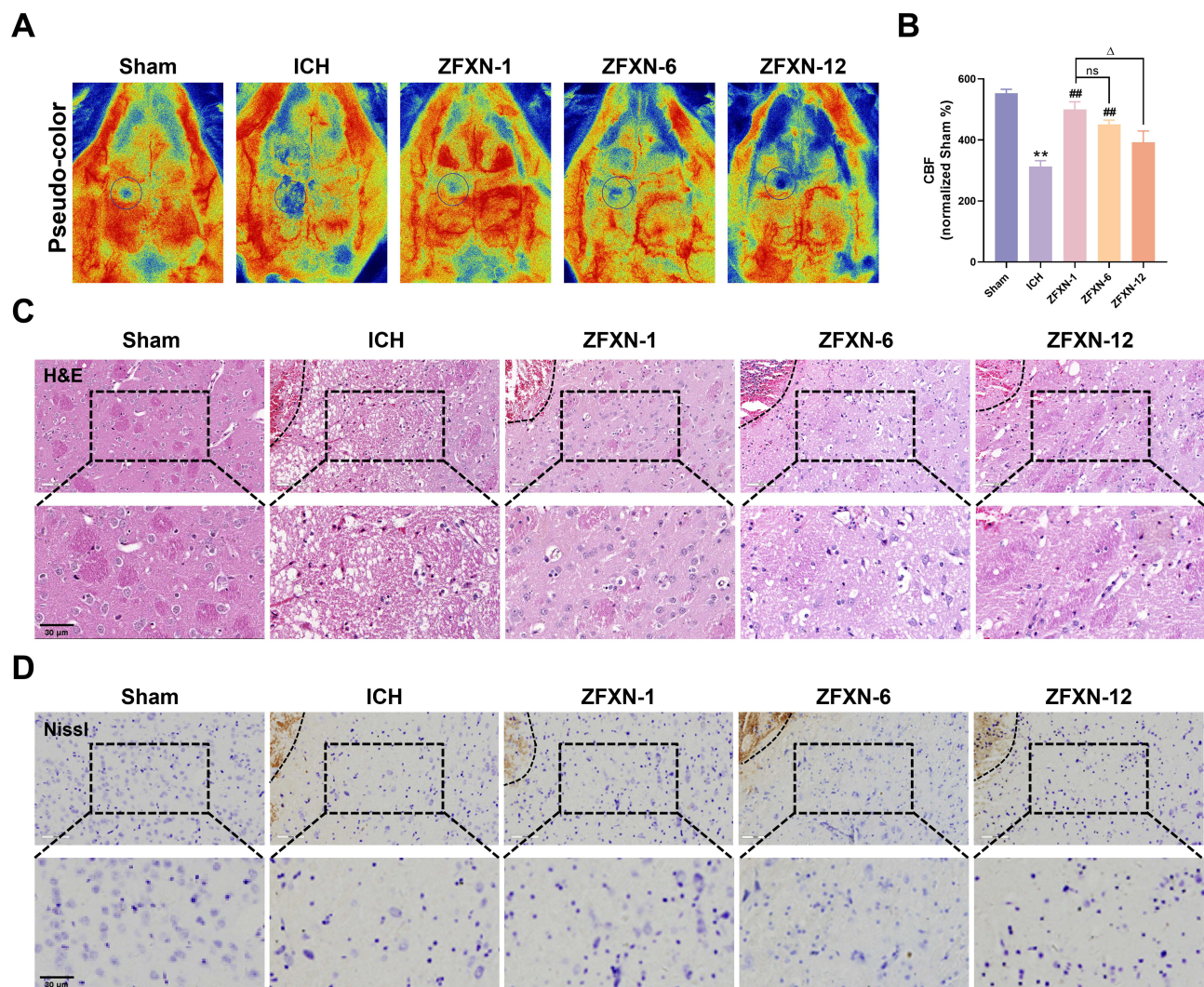


**Figure 2** ZFXN alleviated neurological impairment induced by ICH in rats. **(A and B)** Representative CBF images using laser speckle imaging system and quantification, the circle is the needle entry point (n=5). **(C)** Representative images of H&E staining (n=5. Scale bar=100  $\mu$ m in upper panel; Scale bar=30  $\mu$ m in lower panel) **(D)** Representative images of Nissl staining (n=5. Scale bar=100  $\mu$ m in upper panel; Scale bar=30  $\mu$ m in lower panel). \*\* $p$ <0.01 vs Sham group; ### $p$ <0.01 vs ICH group;  $\Delta$  $p$ <0.05; ns indicates no significant difference ( $p$ ≥0.05).

## ZFXN Inhibited NF- $\kappa$ B/NLRP3 Axis Surrounding Hematoma in ICH Rats

The activated NF- $\kappa$ B/NLRP3 axis causes the body to release pro-inflammatory cytokines after ICH such as IL-1 $\beta$  and TNF- $\alpha$ , thereby leading to neuroinflammatory response.<sup>20,38,39</sup> Our results demonstrated a significant decrease in cytosol levels of NF- $\kappa$ B-p65 around the hematoma 24 hours post-ICH, however its levels in nucleus were significantly increased. Nevertheless, these alterations in NF- $\kappa$ B-p65 were markedly restored by ZFXN-1 treatment (Figure 5A and B). Furthermore, the IF intensity of NLRP3, ASC, and Cleaved Cysteine aspartate-specific protease-1 (Caspase-1) surrounding the hematoma in ICH rats was significantly elevated compared with Sham rats, while these levels were markedly decreased in ZFXN-1 rats (Figure 5C–F). Finally, the protein expression levels of NLRP3, ASC and C-Casp1 around the hematoma in ICH rats were higher than those of in Sham rats, however, their levels were lower in ZFXN-1 rats than those of in ICH rats (Figure 5G–H). These findings indicate ZFXN administration one-hour after ICH suppresses the neuroinflammatory response surrounding the hematoma by inhibiting the NF- $\kappa$ B/NLRP3 axis.



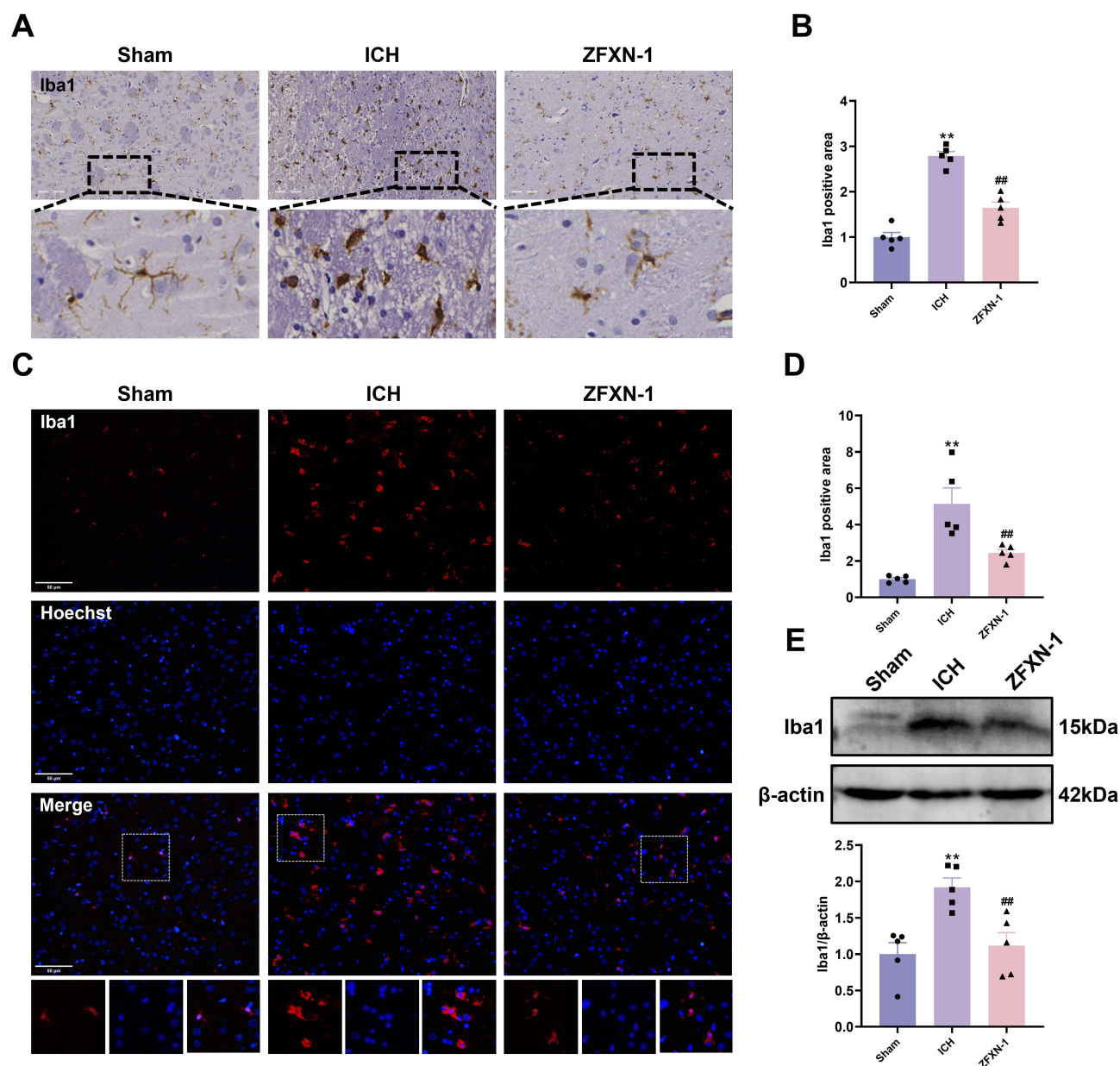


**Figure 3** ZFXN inhibited microglial activation around the hematoma in ICH rats. (A and B) Representative immunohistochemical staining images of Iba1 and quantification (Scale bar=100  $\mu$ m in upper panel; 4 $\times$ magnification in lower panel, n=5). (C and D) Representative IF staining images of Iba1 IF staining and quantification (Scale bar=100  $\mu$ m in upper panel; 1.6 $\times$  magnification in lower panel, n=5). (E) Representative WB bands of Iba1 and quantification (n=5). \*\* $p$ <0.01 vs Sham group; ## $p$ <0.01 vs ICH group.

## ZFXN Inhibited the NF- $\kappa$ B/NLRP3 Axis in LPS-Treated BV-2 Cells

Microglial activation contributes to neuroinflammation impairment post-ICH.<sup>13</sup> Our data indicated that ZFXN did not affect the viability of BV-2 cells within the concentration range of 0.625–160  $\mu$ g/mL (Figure 6A), while LPS markedly decreased cell viability in a dose-dependent fashion (Figure 6B). ZFXN significantly increased cell viability in LPS-induced BV-2 cells in a dose-dependent manner (Figure 6C). In the present study, BV-2 cells were treated with 2  $\mu$ M LPS for 12 hours, followed by the addition of 5  $\mu$ g/mL ZFXN for additional 12 hours. IF analysis revealed that ZFXN significantly reduced nuclear levels of NF- $\kappa$ B-p65 compared with LPS-treated cells (Figure 6D and E). Concurrently, ZFXN markedly decreased the protein levels of NLRP3, ASC, and Cleaved Caspase-1 in LPS-treated BV-2 cells (Figure 6F and G). These results suggest ZFXN inhibits LPS-induced microglial activation by suppressing NF- $\kappa$ B/NLRP3 axis.

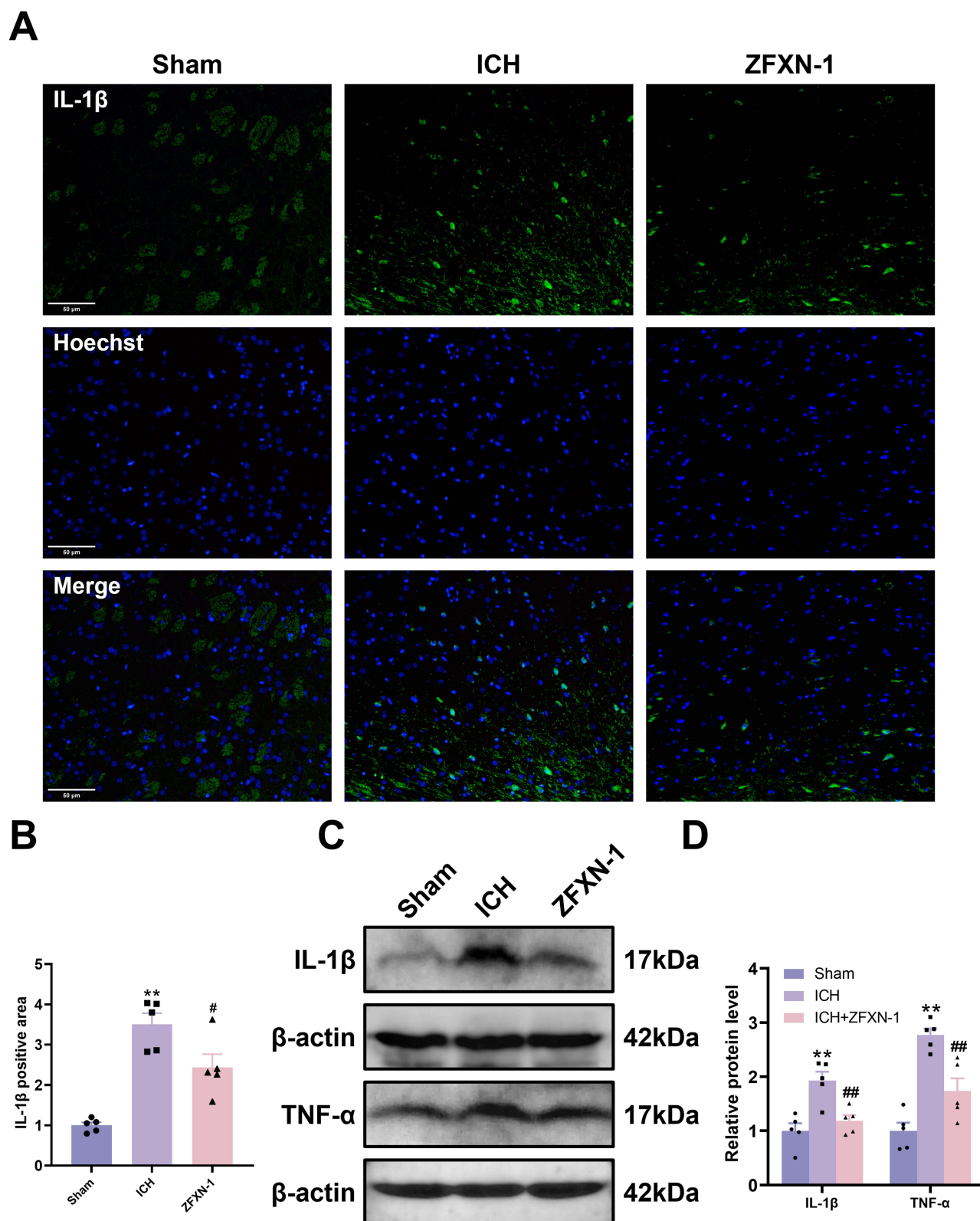


**Figure 4** ZFXN suppressed inflammatory cytokines in the perihematoma area of ICH rats. (**A** and **B**) Representative IF images of IL-1 $\beta$  in the perihematoma area and quantification (Scale bar=100  $\mu$ m, n=5) (**C** and **D**) Representative WB images of IL-1 $\beta$  and TNF- $\alpha$  in the peri-hematoma area and quantification (n=5). \*\* $p$ <0.01 vs Sham group; # $p$ <0.05, ## $p$ <0.01 vs ICH group.



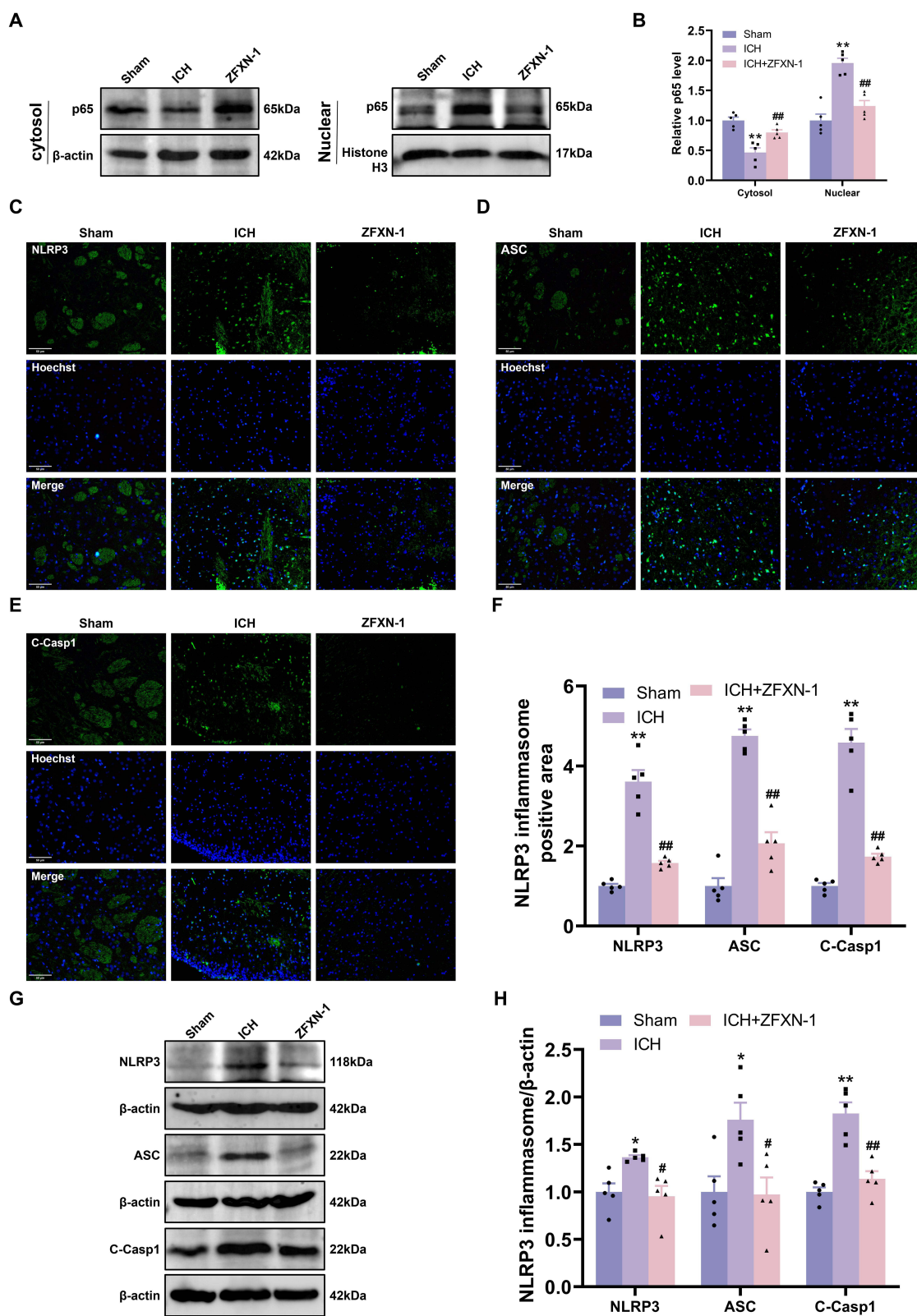


**Figure 5** ZFXN inhibited NF- $\kappa$ B/NLRP3 axis surrounding the hematoma in ICH rats. (**A** and **B**) Representative WB images of NF- $\kappa$ B-p65 in cytosol and nuclear fractions and quantification (n=5). (**C**–**F**) Representative IF images of NLRP3, ASC and Cleaved Caspase-1 and quantification (scale bar=100  $\mu$ m, n=5). (**G** and **H**) Representative WB images of NLRP3, ASC and Cleaved Caspase-1 and quantification (n=5). \* $p$ <0.01, \*\* $p$ <0.01 vs Sham group; # $p$ <0.01, ## $p$ <0.01 vs ICH group.

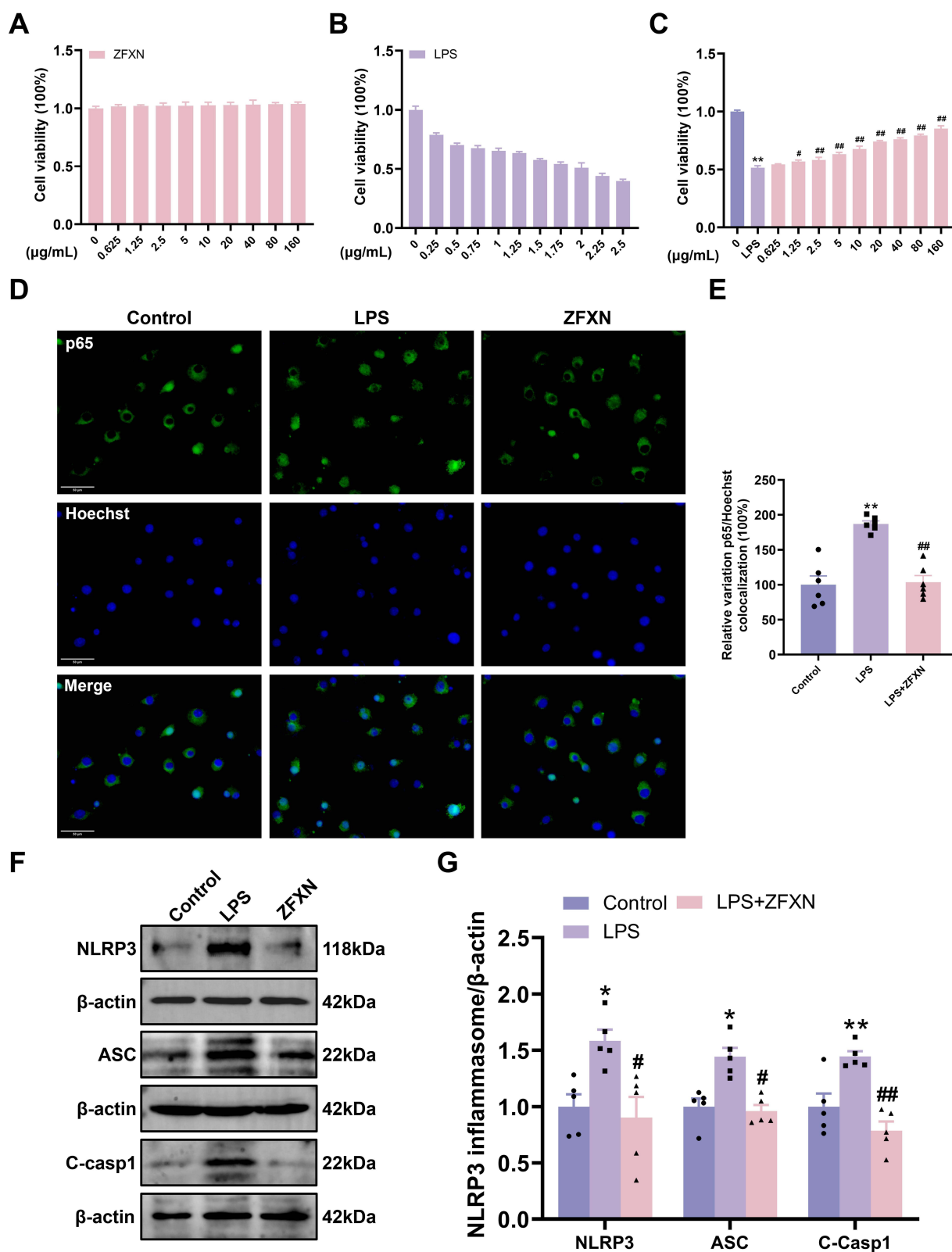


**Figure 6** ZFXN inhibited the NF- $\kappa$ B/NLRP3 axis in LPS-treated BV-2 cells. **(A)** Effects of ZFXN on cell viability of BV-2 ( $n=6$ ). **(B)** Effect of LPS on cell viability of BV-2 ( $n=6$ ). **(C)** Effects of ZFXN on cell viability of 2  $\mu\text{M}$  LPS-treated BV-2 cells for 24h ( $n=6$ ). **(D and E)** Representative IF images of NF- $\kappa$ B-p65 and quantification (scale bar=100  $\mu\text{m}$ ,  $n=6$ ). **(F and G)** Representative WB images of NLRP3, ASC and Cleaved Caspase-1 and quantification ( $n=5$ ). \* $p<0.05$ , \*\* $p<0.01$  vs control group; # $p<0.05$ , ## $p<0.01$  vs LPS-group.

## Discussion

ZFXN demonstrates distinct therapeutic advantages over conventional anti-inflammatory approaches through its unique polypharmacological profile.<sup>40,41</sup> Unlike single-target agents that merely suppress inflammatory cascades, ZFXN orchestrates a coordinated neuroprotective response by simultaneously inhibiting NF- $\kappa$ B nuclear translocation (reducing pro-inflammatory cytokine production), disrupting NLRP3 inflammasome assembly (blocking IL-1 $\beta$ /IL-18 maturation) and activating endogenous repair mechanisms (enhancing neurotrophic factor expression). These findings suggest that incorporating ZFXN into ultra-early (<6 h) ICH treatment protocols may extend the therapeutic window, particularly in primary care settings where immediate hematoma evacuation is unavailable, thus establishing a novel paradigm for combined pharmacological and surgical interventions during the “golden hour”.

The volume and expansion of hematoma post-ICH are closely related to short-term mortality, disability, and long-term prognosis. Therefore, limiting and preventing hematoma expansion is considered as a primary therapeutic target in clinical.<sup>4,42</sup> Given the nonregenerative nature of neuronal cells, mitigating neurological injury in the early stage of post-ICH is essential to preserving the quality of life in surviving patients.<sup>43,44</sup> Our results demonstrate that ZFXN administration at one- and six-hours post-ICH not only reduced hematoma volume at 24-hours, but also improved scores in mNSS, Bederson and Zea Longa tests, alongside a reduction in neuronal impairment surrounding the hematoma (Figures 1 and 2). These findings suggest ZFXN is beneficial for short-term outcomes following ICH when administered orally within six hours, particularly within the first hour post-ICH.

Microglia-driven neuroinflammation is associated with hematoma expansion and secondary damage following ICH.<sup>38,45</sup> Inflammation is currently regarded as a reliable predictor of hematoma expansion in the early stage and prognosis in patients with ICH and is also considered a potential target for early intervention.<sup>13,46</sup> As resident macrophages of the brain, microglia become activated in the periphery of hematoma post-ICH and secrete cytokines including IL-1 $\beta$  and TNF- $\alpha$ , which are implicated in the neuroinflammatory processes that occur in the vicinity of hematomas.<sup>45,47</sup> Furthermore, a reduction in CBF is a significant contributor to microglial activation and neuroinflammation in the peripheral regions of hematomas, which is exacerbated by increased intracranial pressure following ICH.<sup>48</sup> Our research indicates that the administration of ZFXN at one- and six-hour post-ICH significantly enhances CBF at the 24-hour mark in ICH rat models (Figure 2). Additionally, early oral administration of ZFXN at one hours post-ICH resulted in decreased microglial activation and lower levels of the levels of IL-1 $\beta$  and TNF- $\alpha$  around the hematoma (Figures 3 and 4). These results suggest ZFXN administration at one hours post-ICH mitigates neuroinflammation surrounding the hematoma by inhibiting microglial activation.

Inflammatory cytokines such as IL-1 $\beta$  and TNF- $\alpha$  activate the NF- $\kappa$ B signaling pathway in microglia, leading to the activation of NLRP3 inflammasome, which is closely associated with neuroinflammation responses. The NLRP3 inflammasome can be activated following the nuclear translocation of NF- $\kappa$ B-p65, recognized as the principal transcription factor governing the NLRP3 inflammasome.<sup>49,50</sup> Increasing evidences support the activation of NF- $\kappa$ B and NLRP3 inflammasome in microglia after ICH, contributing to neuroinflammation and neurological injury.<sup>51,52</sup> Certain bioactive compounds, including ursolic acid, isoliquiritigenin, and isoquercitrin, have been shown to alleviate neuroinflammation and neural impairment following ICH.<sup>18,20,53</sup> In the current study, we observed that ZFXN administration at one-hour post-ICH not only inhibited the nuclear translocation levels of NF- $\kappa$ B-p65 in ICH rats and LPS-treated BV-2 cells, but also suppressed the activation of NLRP3 inflammasome, as evidenced by reduced IF intensity and protein expression levels of NLRP3, ASC and Cleaved Caspase-1 following ZFXN treatment (Figures 5 and 6). These results suggest ZFXN administration at one-hour post-ICH inhibits neuroinflammation response in the periphery of hematoma post-ICH by targeting NF- $\kappa$ B/NLRP3 axis.

This study has two primary limitations: First, the observed short-term benefits of ultra-early ZFXN administration following ICH necessitate validation through multicenter randomized placebo-controlled double-blind trials. Second, the exclusive focus on 24-hour post-ICH outcomes precludes evaluation of long-term functional recovery and secondary complications, thereby restricting comprehensive interpretation of the intervention's potential neuroprotective mechanisms. Future studies will incorporate extended observation windows to systematically investigate sustained neuroprotective effects of the intervention.

## Conclusion

This work provides the first evidence that ZFXN administration within six hours post-ICH can alleviate acute neurological dysfunctions in rat models, particularly when administered at one-hour post-ICH. The primary mechanism underlying this effect appears to be the reduction of neuroinflammation surrounding the hematoma by inhibiting NF- $\kappa$ B/NLRP3 axis. These findings offer potential insights into improving short-term outcomes in ICH patients through early ZFXN administration. ZFXN demonstrates preclinical efficacy in modulating the NF- $\kappa$ B/NLRP3 pathway for intracerebral hemorrhage (ICH), yet translational challenges persist due to interspecies pathophysiological disparities, limitations of standardized animal models in replicating clinical comorbidities, and discordance between preclinical functional assessments and human-relevant outcomes, necessitating validation through biomarker-stratified RCTs with clinically aligned endpoints.

## Acknowledgments

This work was supported by Science & Technology Department of Sichuan Province (Grant No. 2019YFS0040) and the Improvement plan of “Xinglin scholar” scientific research talent, Chengdu University of Traditional Chinese Medicine (No. XKTD2022002).

## Author Contributions

All authors made a significant contribution to the work reported, whether that is in the conception, study design, execution, acquisition of data, analysis and interpretation, or in all these areas; took part in drafting, revising or critically reviewing the article; gave final approval of the version to be published; have agreed on the journal to which the article has been submitted; and agree to be accountable for all aspects of the work.

## Disclosure

The authors declare no competing interests in this work.

## References

1. Puy L, Parry-Jones AR, Sandset EC, Dowlatabadi D, Ziai W, Cordonnier C. Intracerebral haemorrhage. *Nat Rev Dis Prim.* 2023;9(1):14. doi:10.1038/s41572-023-00424-7
2. Lattanzi S, Di Napoli M, Ricci S, Divani AA. Matrix metalloproteinases in acute intracerebral hemorrhage. *Neurotherapeutics.* 2020;17(2):484–496. doi:10.1007/s13311-020-00839-0
3. Seiffge DJ, Anderson CS. Treatment for intracerebral hemorrhage: dawn of a new era. *Int J Stroke.* 2024;19(5):482–489. doi:10.1177/17474930241250259
4. Pradilla G, Ratcliff JJ, Hall AJ, et al. Trial of early minimally invasive removal of intracerebral hemorrhage. *New Engl J Med.* 2024;390(14):1277–1289. doi:10.1056/NEJMoa2308440
5. Connolly SJ, Sharma M, Cohen AT, et al. Andexanet for factor xa inhibitor–associated acute intracerebral hemorrhage. *New Engl J Med.* 2024;390(19):1745–1755. doi:10.1056/NEJMoa2313040
6. Ali M, Smith C, Vasan V, et al. Management of intracavitary bleeding during ultra-early minimally invasive intracerebral hemorrhage evacuation. *J Neurosurg.* 2024;1(aop):1–11. doi:10.3171/2024.6.JNS232985
7. Houskamp EJ, Liu Y, Silva Pinheiro Do Nascimento J, et al. P2Y12 inhibitor use predicts hematoma expansion in patients with intracerebral hemorrhage. *Ann Clin Transl Neurol.* 2024;11(6):1535–1540. doi:10.1002/acn3.52070
8. Yakhkind A, Yu W, Li Q, Goldstein JN, Mayer SA. Code-ICH: a new paradigm for emergency intervention. *Curr Neurol Neurosci Rep.* 2024;24(9):365–371. doi:10.1007/s11910-024-01364-9
9. Duan T, Li L, Yu Y, et al. Traditional Chinese medicine use in the pathophysiological processes of intracerebral hemorrhage and comparison with conventional therapy. *Pharmacol Res.* 2022;179:106200. doi:10.1016/j.phrs.2022.106200
10. Shao A, Zhu Z, Li L, Zhang S, Zhang J. Emerging therapeutic targets associated with the immune system in patients with intracerebral haemorrhage (ICH): from mechanisms to translation. *EBioMedicine.* 2019;45:615–623. doi:10.1016/j.ebiom.2019.06.012
11. Fan L, Jin L, Tang T, et al. Neutrophil-like pH-responsive pro-erythrophagocytic nanoparticles improve neurological recovery by promoting erythrophagocytosis after intracerebral hemorrhage. *Theranostics.* 2024;14(1):283–303. doi:10.7150/thno.90370
12. Morotti A, Boulouis G, Dowlatabadi D, et al. Intracerebral haemorrhage expansion: definitions, predictors, and prevention. *Lancet Neurol.* 2023;22(2):159–171. doi:10.1016/S1474-4422(22)00338-6
13. Xue M, Yong VW. Neuroinflammation in intracerebral haemorrhage: immunotherapies with potential for translation. *Lancet Neurol.* 2020;19(12):1023–1032. doi:10.1016/S1474-4422(20)30364-1
14. Zhu W, Zhou J, Ma B, Fan C. Predictors of early neurological deterioration in patients with intracerebral hemorrhage: a systematic review and meta-analysis. *J Neurol.* 2024;271(6):2980–2991. doi:10.1007/s00415-024-12230-6
15. Tsai HH, Hsieh YC, Lin JS, et al. Functional investigation of meningeal lymphatic system in experimental intracerebral hemorrhage. *Stroke.* 2022;53(3):987–998. doi:10.1161/STROKEAHA.121.037834



16. Wang Y, Tian M, Tan J, et al. Irisin ameliorates neuroinflammation and neuronal apoptosis through integrin  $\alpha\text{V}\beta 5$ /AMPK signaling pathway after intracerebral hemorrhage in mice. *J Neuroinflammation*. 2022;19:82. doi:10.1186/s12974-022-02438-6
17. Liu C, Yao K, Tian Q, et al. CXCR4-BTK axis mediate pyroptosis and lipid peroxidation in early brain injury after subarachnoid hemorrhage via NLRP3 inflammasome and NF- $\kappa$ B pathway. *Redox Biol*. 2023;68:102960. doi:10.1016/j.redox.2023.102960
18. Guo T, Chen G, Yang L, Deng J, Pan Y. Piezo1 inhibitor isoquercitrin rescues neural impairment mediated by NLRP3 after intracerebral hemorrhage. *Exp Neurol*. 2024;379:114852. doi:10.1016/j.expneurol.2024.114852
19. Zhong X, Wang Y, Hu D, Ning Z, Deng M. Investigation of the mitophagy mechanism underlying Zhongfeng Xingnao liquid in collagenase-induced cerebral hemorrhage mouse model. *J Li-Shizhen Trad Chi Med*. 2024;35(3):584–588.
20. Lei P, Li Z, Hua Q, et al. Ursolic acid alleviates neuroinflammation after intracerebral hemorrhage by mediating microglial pyroptosis via the NF- $\kappa$ B/NLRP3/GSDMD pathway. *Int J Mol Sci*. 2023;24(19):14771. doi:10.3390/ijms241914771
21. Yang W, Wen W, Chen H, et al. Zhongfeng Xingnao Liquid ameliorates post-stroke cognitive impairment through sirtuin1 (SIRT1)/nuclear factor erythroid 2-related factor 2 (Nrf2)/heme oxygenase 1 (HO-1) pathway. *Chin J Nat Med*. 2025;23(1):77–89. doi:10.1016/S1875-5364(25)60808-9
22. Xia D, Yuan J, Wu D, Dai H, Zhuang Z. Salvianolic acid B ameliorates neuroinflammation and neuronal injury via blocking NLRP3 inflammasome and promoting SIRT1 in experimental subarachnoid hemorrhage. *Front Immunol*. 2023;14:1159958. doi:10.3389/fimmu.2023.1159958
23. Zhang X, Cai Y, Chen M, et al. Danshen-chuanxiong-honghua ameliorates neurological function and inflammation in traumatic brain injury in rats via modulating ghrelin/GHSR. *J Ethnopharmacol*. 2025;345:119625. doi:10.1016/j.jep.2025.119625
24. Guo S. *A multicenter, double-blind, randomized placebo-controlled trial on the safety and efficacy of Zhongfengxingnao Formula in the treatment of moderate and severe intracerebral hemorrhage*. MA thesis. Chengdu University of traditional Chinese medicine; 2023. doi:10.26988/d.cnki.gcdzu.2023.000791.
25. Guo J, Chen X, Wu M, et al. Traditional Chinese medicine FYTF-919 (Zhongfeng Xingnao oral prescription) for the treatment of acute intracerebral haemorrhage: a multicentre, randomised, placebo-controlled, double-blind, clinical trial. *Lancet*. 2024;404(10468):2187–2196. doi:10.1016/S0140-6736(24)02261-X
26. Pensato U, Tanaka K, Ospel J, et al. Validation of the black-&-white sign to predict intracerebral hematoma expansion in the multi-center PREDICT study cohort. *Int J Stroke*. 2024;17474930241307466. doi:10.1177/17474930241307466
27. Nath FP, Kelly PT, Jenkins A, Mendelow AD, Graham DI, Teasdale GM. Effects of experimental intracerebral hemorrhage on blood flow, capillary permeability, and histochemistry. *J Neurosurg*. 1987;66(4):555–562. doi:10.3171/jns.1987.66.4.0555
28. Yang YP, Liu XP, Tai LW. The skills to model intracerebral hemorrhage by infusing autologous blood in rats. *Acta Neuropharmacologica*. 2012;2(2):29–31.
29. Li Z, Li M, Shi SX, et al. Brain transforms natural killer cells that exacerbate brain edema after intracerebral hemorrhage. *J Exp Med*. 2020;217(12):e20200213. doi:10.1084/jem.20200213
30. Bederson JB, Pitts LH, Tsuji M, Nishimura MC, Davis RL, Bartkowski H. Rat middle cerebral artery occlusion: evaluation of the model and development of a neurologic examination. *Stroke*. 1986;17(3):472–476. doi:10.1161/01.STR.17.3.472
31. Longa EZ, Weinstein PR, Carlson S, Cummins R. Reversible middle cerebral artery occlusion without craniectomy in rats. *Stroke*. 1989;20(1):84–91. doi:10.1161/01.STR.20.1.84
32. Vu EL, Brown CH, Brady KM, Hogue CW. Monitoring of cerebral blood flow autoregulation: physiologic basis, measurement, and clinical implications. *Br J Anaesth*. 2024;132(6):1260–1273. doi:10.1016/j.bja.2024.01.043
33. Yu W, Che C, Yang Y, et al. Bioactive self-assembled nanoregulator enhances hematoma resolution and inhibits neuroinflammation in the treatment of intracerebral hemorrhage. *Adv Sci*. 2024:e2408647. doi:10.1002/adv.202408647
34. Jones OA, Mohamed S, Hinz R, et al. Neuroinflammation and blood-brain barrier breakdown in acute, clinical intracerebral hemorrhage. *J Cereb Blood Flow Metab*. 2024;271678X241274685. doi:10.1177/0271678X241274685
35. Almarghalani DA, Bahader GA, Ali M, Tillekeratne LMV, Shah ZA. Cofilin inhibitor improves neurological and cognitive functions after intracerebral hemorrhage by suppressing endoplasmic reticulum stress related-neuroinflammation. *Pharmaceuticals*. 2024;17(1):114. doi:10.3390/ph17010114
36. Seiffge DJ, Fandler-Höfler S, Du Y, et al. Intracerebral haemorrhage — mechanisms, diagnosis and prospects for treatment and prevention. *Nat Rev Neurol*. 2024;20(12):708–723. doi:10.1038/s41582-024-01035-w
37. Wang M, Ye X, Hu J, et al. NOD1/RIP2 signalling enhances the microglia-driven inflammatory response and undergoes crosstalk with inflammatory cytokines to exacerbate brain damage following intracerebral haemorrhage in mice. *J Neuroinflammation*. 2020;17(1):364. doi:10.1186/s12974-020-02015-9
38. Ohashi SN, DeLong JH, Kozberg MG, et al. Role of inflammatory processes in hemorrhagic stroke. *Stroke*. 2023;54(2):605–619. doi:10.1161/STROKEAHA.122.037155
39. Zhang Z, Zhang Z, Lu H, Yang Q, Wu H, Wang J. Microglial polarization and inflammatory mediators after intracerebral hemorrhage. *Mol Neurobiol*. 2017;54(3):1874–1886. doi:10.1007/s12035-016-9785-6
40. Wang Y, Yin Y, Liu Y, et al. Notoginsenoside R1 treatment facilitated Nrf2 nuclear translocation to suppress ferroptosis via Keap1/Nrf2 signaling pathway to alleviated high-altitude myocardial injury. *Biomed Pharmacother*. 2024;175:116793. doi:10.1016/j.biopha.2024.116793
41. Tang K, Qin W, Wei R, et al. Ginsenoside Rd ameliorates high glucose-induced retinal endothelial injury through AMPK-STR1 interdependence. *Pharmacol Res*. 2022;179:106123. doi:10.1016/j.phrs.2022.106123
42. Hanley DF, Ziai WC, Vahidy FS, et al. Intracerebral hemorrhage: keep it simple. *Stroke*. 2024;55(12):2942–2945. doi:10.1161/STROKEAHA.124.048533
43. Zhou JF, Xiong Y, Kang X, et al. Application of stem cells and exosomes in the treatment of intracerebral hemorrhage: an update. *Stem Cell Res Ther*. 2022;13(1):281. doi:10.1186/s13287-022-02965-2
44. Li XN, Lin L, Li XW, et al. BSA-stabilized selenium nanoparticles ameliorate intracerebral hemorrhage's-like pathology by inhibiting ferroptosis-mediated neurotoxicology via Nrf2/GPX4 axis activation. *Redox Biol*. 2024;75:103268. doi:10.1016/j.redox.2024.103268
45. Tschoe C, Bushnell CD, Duncan PW, Alexander-Miller MA, Wolfe SQ. Neuroinflammation after intracerebral hemorrhage and potential therapeutic targets. *J Stroke*. 2020;22(1):29–46. doi:10.5853/jos.2019.02236
46. Chu H, Huang C, Zhou Z, Tang Y, Dong Q, Guo Q. Inflammatory score predicts early hematoma expansion and poor outcomes in patients with intracerebral hemorrhage. *Int J Surg*. 2023;109(3):266–276. doi:10.1097/JS9.0000000000000191



47. Ren H, Pan Y, Wang D, et al. CD22 blockade modulates microglia activity to suppress neuroinflammation following intracerebral hemorrhage. *Pharmacol Res.* **2023**;196:106912. doi:10.1016/j.phrs.2023.106912
48. Zhang J, Zhu Q, Wang J, et al. Mitochondrial dysfunction and quality control lie at the heart of subarachnoid hemorrhage. *Neural Regen Res.* **2024**;19(4):825–832. doi:10.4103/1673-5374.381493
49. Li S, Fang Y, Zhang Y, et al. Microglial NLRP3 inflammasome activates neurotoxic astrocytes in depression-like mice. *Cell Rep.* **2022**;41(4):111532. doi:10.1016/j.celrep.2022.111532
50. Zhao Y, Shao C, Zhou H, et al. Salvianolic acid B inhibits atherosclerosis and TNF- $\alpha$ -induced inflammation by regulating NF- $\kappa$ B/NLRP3 signaling pathway. *Phytomedicine.* **2023**;119:155002. doi:10.1016/j.phymed.2023.155002
51. Palahati A, Luo Y, Qin L, et al. TonEBP: a key transcription factor in microglia following intracerebral hemorrhage induced-neuroinflammation. *Int J Mol Sci.* **2024**;25(3):1438. doi:10.3390/ijms25031438
52. Fang M, Xia F, Wang J, et al. The NLRP3 inhibitor, OLT1177 attenuates brain injury in experimental intracerebral hemorrhage. *Int Immunopharmacol.* **2024**;131:111869. doi:10.1016/j.intimp.2024.111869
53. Zeng J, Chen Y, Ding R, et al. Isoliquiritigenin alleviates early brain injury after experimental intracerebral hemorrhage via suppressing ROS- and/or NF- $\kappa$ B-mediated NLRP3 inflammasome activation by promoting Nrf2 antioxidant pathway. *J Neuroinflammation.* **2017**;14(1):119. doi:10.1186/s12974-017-0895-5

## Journal of Inflammation Research

### Publish your work in this journal

The Journal of Inflammation Research is an international, peer-reviewed open-access journal that welcomes laboratory and clinical findings on the molecular basis, cell biology and pharmacology of inflammation including original research, reviews, symposium reports, hypothesis formation and commentaries on: acute/chronic inflammation; mediators of inflammation; cellular processes; molecular mechanisms; pharmacology and novel anti-inflammatory drugs; clinical conditions involving inflammation. The manuscript management system is completely online and includes a very quick and fair peer-review system. Visit <http://www.dovepress.com/testimonials.php> to read real quotes from published authors.

Submit your manuscript here: <https://www.dovepress.com/journal-of-inflammation-research-journal>

**Dovepress**  
Taylor & Francis Group